Radial basis functions with compact support for elastic registration of medical images

M. Fornefett*, K. Rohr, H.S. Stiehl

Universität Hamburg, Fachbereich Informatik, Arbeitsbereich Kognitive Systeme, Vogt-Kölln-Str. 30, D-22527 Hamburg, Germany

Abstract

Common elastic registration schemes based on landmarks and radial basis functions (RBFs) such as thin-plate splines or multiquadrics are global. Here, we introduce radial basis functions with compact support for elastic registration of medical images which have an improved locality, i.e. which allow to constrain elastic deformations to image parts where required. We give the theoretical background of these basis functions and compare them with other basis functions w.r.t. locality, solvability, and efficiency. A detailed comparison with the Gaussian as well as conditions for preserving topology is given. An important property of the used RBFs (Wendland's ψ-functions) is that they are positive definite. Therefore, in comparison to the use of the truncated Gaussian, the solvability of the resulting system of equations is always guaranteed. We demonstrate the applicability of our approach for synthetic as well as for (two-dimensional) 2D and 3D tomographic images. © 2000 Elsevier Science B.V. All rights reserved.

Keywords: Elastic registration; Radial basis function; Compact support

1. Introduction

Registration is an important technique in medical image analysis. Rigid and affine registration methods can only cope with global differences, for example, translation, rotation, and scaling. In many cases, however, elastic or non-rigid methods are required to cope with local differences between the images. Such differences are due to, for example, scanner-induced deformations, movements of the patient, surgical interventions, or different anatomy (e.g. image atlas-registration).

In this paper, we consider a point-based elastic registration approach based on radial basis functions (RBFs). With this approach the transformation is composed of radially symmetric functions that serve as basis functions. The choice of the type of the RBF is crucial for the overall characteristics such as the smoothness or the locality of the transformation function.

Bookstein [2] has introduced thin-plate splines for medical image registration. This approach yields minimal bending energy properties measured over the whole image, but the deformation is not limited to regions where the point landmarks are placed. This behaviour is advantageous for

yielding an overall smooth deformation, but it is problematic when rather local deformations limited to image parts are desired. To cope with local deformations, the landmarks have to be well distributed over the images to prevent deformations in regions where no changes are desired [1].

Others have investigated multiquadrics as RBFs for registration, e.g. [11], and for image deformations [15]. These RBFs have a parameter which controls their locality. However, the function values of multiquadrics are increasing with growing distance from the landmark position and thus the registration result at locations far off the center of the RBFs is largely influenced. Other RBFs decrease with growing distance from the landmark position such as inverse multiquadrics, e.g. [15], and the Gaussian, e.g. [1]. Since these RBFs asymptotically approach zero, the global influence is reduced, but it is not spatially limited, i.e. these RBFs have no compact support. In Ref. [8], a local registration approach has been described, where polynomials with spatially local weight functions have been used, but where the distribution of landmarks must satisfy certain requirements to avoid the appearance of holes in the transformed images.

In this paper, we introduce RBFs with compact support for the registration of medical images. The basis functions we employ have a similar shape as the Gaussian, but they have the advantage that their influence is limited around a

---

* Corresponding author.
  E-mail address: fornefett@informatik.uni-hamburg.de (M. Fornefett).

landmark (in 2D and 3D images on a circle or a sphere, respectively). This property allows the registration of medical images where changes occur only locally. The application scenario we have in mind is the registration of local changes in medical images due to the resection of a tumor or due to other surgical interventions. Our approach has also very nice theoretical properties. Actually, for the basis functions we use, it can be shown that the resulting system of equations is always solvable. Thus, we provide an answer to a previously posed question in Ref. [1], where Gaussian-shaped RBFs with compact support are sought while solvability is always ensured.

Below, we first give an overview of the general scheme for registration based on RBFs (Section 2). In Section 3, we introduce an elastic registration scheme using RBFs with compact support and describe its properties. Finally, in Section 4, we present experimental results for 2D and 3D images. Parts of this work have previously been published in Refs. [5,6].

2. Image registration with RBFs

In this section, we briefly describe the radial basis function approach and discuss its properties depending on the choice of the basis function.

2.1. General scheme

Generally, in registration applications one has to determine a transformation function $\mathbf{u} : \mathbb{R}^d \to \mathbb{R}^d$, where d is the image dimension, e.g. $d = 2, 3$ for 2D and 3D images, respectively. An interpolation transformation function $u(\mathbf{x})$ based on point-landmarks must fulfill the following constraints:

$$\mathbf{u}(\mathbf{p}_i) = \mathbf{q}_i, \qquad i = 1...n, \tag{1}$$

where $\mathbf{p}_i \in \mathbb{R}^d$ constitute a given set of point-landmarks in the source image and $\mathbf{q}_i \in \mathbb{R}^d$ are the corresponding landmarks in the target image. Often, each coordinate of the transformation function is calculated separately, i.e. the interpolation problem $u_k : \mathbb{R}^d \to \mathbb{R}$ is solved for each coordinate $k = 1...d$ with the corresponding constraints $u_k(\mathbf{p}_i) = \mathbf{q}_{i,k}$. In the following, we write $u(\mathbf{x})$ instead of $u_k(\mathbf{x})$. In 2D, $u(\mathbf{x})$ is calculated separately for $u_1(\mathbf{x})$ and $u_2(\mathbf{x})$ and in 3D for $u_1(\mathbf{x})$, $u_2(\mathbf{x})$, and $u_3(\mathbf{x})$.

If we apply a radial basis function approach, then the interpolation function $u(\mathbf{x})$ generally consists of two parts.

$$u(\mathbf{x}) = \phi_s(\mathbf{x}) + R_s(\mathbf{x}), \tag{2}$$

where $\phi_s(\mathbf{x})$ is a sum of polynomials up to degree p and $R_s(\mathbf{x})$ consists of a sum of RBFs (the index s denotes sum):

$$\phi_s(\mathbf{x}) = \sum_{j=1}^{M} \beta_j \phi_j(\mathbf{x}), \qquad R_s(\mathbf{x}) = \sum_{i=1}^{n} \alpha_i R(\|\mathbf{x} - \mathbf{p}_i\|).$$

Here, the $\phi_j(\mathbf{x})$ are a basis of M functions for all polynomials

up to degree p, $R(r) = R(\|\mathbf{r}\|)$ is a function depending only on the distance $r \geq 0$ from the origin, $\|\mathbf{x} - \mathbf{p}_i\| = \|\mathbf{r}\|$ is the Euclidean distance from $\mathbf{x}$ to $\mathbf{p}_i$, and α_i and β_j are coefficients. The RBFs $R(\|\mathbf{x} - \mathbf{p}_i\|)$ are centered around the n landmarks $\mathbf{p}_i$. Inserting Eq. (2) in Eq. (1), and using the following additional constraints:

$$\sum_{i=1}^{n} \alpha_i \phi_j(\mathbf{p}_i) = 0, \qquad j = 1...M,$$

yields the following system of linear equations for the coefficients $\boldsymbol{\alpha} = (\alpha_1, ..., \alpha_n)^{\mathrm{T}}$ and $\boldsymbol{\beta} = (\beta_1, ..., \beta_M)^{\mathrm{T}}$:

$$\begin{pmatrix} \mathbf{K} & \mathbf{P} \\ \mathbf{P}^{\mathrm{T}} & 0 \end{pmatrix} \begin{pmatrix} \boldsymbol{\alpha} \\ \boldsymbol{\beta} \end{pmatrix} = \begin{pmatrix} \mathbf{q}_k \\ 0 \end{pmatrix}, \tag{3}$$

where $\mathbf{K}$ is the $n \times n$ sub-matrix given by $K_{ij} = R(\|\mathbf{p}_i - \mathbf{p}_j\|)$ and $\mathbf{P}$ the $n \times M$ sub-matrix given by $P_{ij} = \phi_j(\mathbf{p}_i)$. $\mathbf{q}_k = (\mathbf{q}_{k,1}, ..., \mathbf{q}_{k,n})^{\mathrm{T}}$ is a vector of the kth coordinate of the target landmarks $\mathbf{q}_i$.

The scheme in Eq. (3) can also be extended to allow for the case of approximation. In this case we have:

$$\begin{pmatrix} \mathbf{K} + \lambda \mathbf{W}^{-1} & \mathbf{P} \\ \mathbf{P}^{\mathrm{T}} & 0 \end{pmatrix} \begin{pmatrix} \boldsymbol{\alpha} \\ \boldsymbol{\beta} \end{pmatrix} = \begin{pmatrix} \mathbf{q}_k \\ 0 \end{pmatrix}$$

$$\tag{4}$$

with

$$\mathbf{W} = \mathrm{diag}\left\{ 1/\sigma_1^2, ..., 1/\sigma_n^2 \right\},$$

where σ_i are the individual weights of the landmarks which represent landmark localization errors and λ is a general weighting parameter. Previously, approximation scheme for elastic registration based on thin-plate splines have been proposed in Refs. [14,13].

2.2. Important properties

The choice of the RBF $R(r)$ determines the characteristics of the transformation function $u(\mathbf{x})$. Given the application scenario from above the following properties are of primary interest:

- *Locality.* By locality we denote the spatial range of influence induced by an additionally used landmark pair. These influences can be rather local, i.e. regions of the registration result at larger distances than a certain radius from the landmark pair do not undergo changes. Alternatively, the landmark pair can influence the whole transformed image. Some RBFs have locality parameters, which allow us to control their influence on the registration result (see also Section 2.3).
- *Solvability.* To find solutions for the coefficients α and β for all possible sets of landmarks, which are not colinear in 2D and not coplanar in 3D, it is required that the matrix on the left-hand side of Eq. (3) has to be non-singular. We will discuss the non-singularity of the matrix based on the choice of the RBF in Section 2.3.

- *Efficiency*. Computational efficiency is important especially for large data sets such as 3D images. The computation of a transformation function depends on the used basis function. Also, for efficiently solving the system (Eq. (3)) it is important whether the involved matrix is dense or sparse.

2.3. Commonly used radial basis functions

A variety of different RBFs have been proposed for elastic image registration and image deformation. These are, for example, thin-plate splines (R_{TPS}) [2,4,14], multiquadrics (R_M) [9,11,15], inverse multiquadrics (R_{IM}) [15], and the Gaussian (R_G) [1]:

$$R_{TPS}(r) = \begin{cases} r^{4-d} \ln r & 4 - d \in 2\mathbb{N} \\ r^{4-d} & \text{otherwise}, \end{cases} \quad (5)$$

$$R_M(r) = (r^2 + c^2)^\mu, \quad \mu \in \mathbb{R}_+, \quad (6)$$

$$R_{IM}(r) = (r^2 + c^2)^{-\mu}, \quad \mu \in \mathbb{R}_+, \quad (7)$$

$$R_G(r) = e^{-r^2/2\sigma^2}. \quad (8)$$

Locality. The first two functions increase, while the latter two functions decrease with growing r from the landmark point. All these functions have in common that they have no compact support and therefore a landmark pair influences the whole registration result.

Solvability. The transformation function (2) has a certain 'polynomial precision', which corresponds to the polynomial part of degree p. Naturally, polynomials have global influence on the registration result. Therefore, to reduce the global influence it would be advantageous to have no polynomial part. Note, that due to a mathematical property of some of these functions, which is the conditional positive definiteness, certain polynomials are necessary to guarantee the non-singularity of the matrix in Eq. (3). For thin-plate splines we have $p = 1(d = 2, 3)$ and for multiquadrics p depends on the exponent μ. The minimal degree p is $p = \lceil \mu \rceil - 1$ where $\lceil \mu \rceil$ denotes the smallest integer $\geq \mu$. The inverse multiquadric and the Gaussian are positive definite, and thus they can be calculated without any polynomial part.

Efficiency. All functions (Eqs. (5)–(8)) involve the calculation of transcendental functions (the logarithm, the exponential, or the square root with $\mu = 0.5$). Also, the matrix in Eq. (3) is always dense since the functions have no compact support.

3. Image registration using RBFs with compact support

The disadvantages of the functions described above are the global influence of a landmark pair on the registration result, the necessary polynomials for some functions, and the necessity of calculating transcendental functions. In this section, we describe a spatially limited RBF which does not have these disadvantages, and is thus suited for our purpose of spatially limited medical image registration.

3.1. ψ-functions of Wendland

We propose to use the ψ-functions of Wendland [17] as RBFs for elastic registration of medical images. These radial basis functions have compact support, are positive definite, and are moreover polynomials. These RBFs have previously been used in Ref. [16] to model facial expressions for videocoding applications. The general form of the RBFs can be stated as:

$$\psi(r) = \begin{cases} p(r) & 0 \leq r \leq 1 \\ 0 & r > 1, \end{cases} \quad (9)$$

where $p(r)$ is a univariate polynomial. Let $\psi(r)$ denote the univariate function, then $\psi : \mathbb{R}^d \to \mathbb{R}, \psi(\|\mathbf{r}\|) = \psi(\|\mathbf{r}\|)$ is the corresponding multivariate function in the space of dimension d. The mathematical property of positive definiteness of ψ depends on the space dimension d. If ψ is positive definite on $\mathbb{R}^d$, then ψ is also positive definite on $\mathbb{R}^g$ with $0 < g \leq d$. It has been proven in Ref. [17] that for given space dimension d and smoothness $C^{2k}(\mathbb{R})$ there exists — up to a constant factor — only one function $\psi(r)$ of the form (9) which is positive definite on $\mathbb{R}^d$ and which has a polynomial of minimal degree $\lfloor d/2 \rfloor + 3k + 1$, where $\lfloor x \rfloor$, the floor function, is the largest integer $\leq x$. This function is given by:

$$\psi_{d,k}(r) := I^k(1 - r)_+^{\lfloor d/2 \rfloor + k + 1}(r) \quad (10)$$

with

$$(1 - r)_+^v = \begin{cases} (1 - r)^v & 0 \leq r < 1 \\ 0 & r \geq 1, \end{cases}$$

as the truncated polynomial and

$$I\psi(r) := \int_r^\infty t\psi(t)\, dt \qquad r \geq 0$$

as the integral operator which is applied k times in Eq. (10). Note, that for even dimensions d, the property $\psi_{d,k} = \psi_{d+1,k}$ holds due to the floor function in Eq. (10). For the functions $\psi_{d,k}(r)$, we chose $d = 3$ which is the largest image dimension in our registration applications. As we have mentioned, the function $\psi_{3,k}$ is positive definite also for smaller dimensions than three. Below, we list ψ-functions for $d = 3$ and $k = 0...2$:

$$\psi_{3,0}(r) = (1 - r)_+^2$$

$$\psi_{3,1}(r) = (1 - r)_+^4(4r + 1)$$

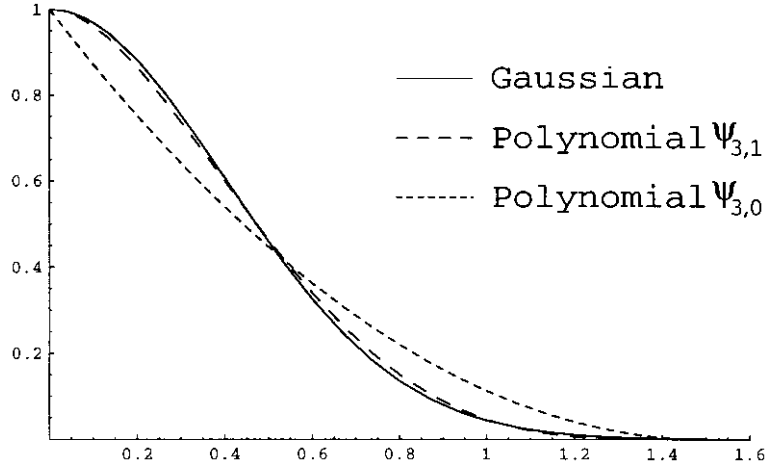$$\psi_{3,2}(r) = (1 - r)_+^6(35r^2 + 18r + 3).$$

Fig. 1. Comparison of $\psi_{a,3,0}$, $\psi_{a,3,1}$ with $a = 1.504$ and the Gaussian with $\sigma = 0.4$. The similarity is apparent.

In Fig. 1, the functions $\psi_{3,0}$ and $\psi_{3,1}$ are plotted together with the Gaussian.

Since we prefer differentiable and smooth functions at $r = 0$, we exclude $k = 0$ and chose the polynomial $\psi_{3,1}$ for $k = 1$ of next smallest degree for use in registration. The mathematical properties also hold for different spatial supports a:

$$\psi_a(r) = \psi(r/a)$$

3.2. Properties of our registration approach

Locality. In our elastic registration approach we first apply a rigid (or affine) transformation function computed by a least squares fit to cope with global differences. Second, we apply the $\psi_{3,1}$-function as RBF together with the identity transformation. These RBFs ensure limited locality of each landmark on a circle or a sphere depending on the length a of the support.

Solvability. The $\psi_{3,1}$-functions are positive definite which ensures that the matrix $\mathbf{K}$ is regular (invertible). Since an additional polynomial part ϕ_s is not necessary, Eq. (3) reduces to:

$$\mathbf{K}\boldsymbol{\alpha} = \mathbf{q}_k. \tag{11}$$

Note, that we use an equal support size a for all landmarks. We are not aware of a theoretical result which states that $\mathbf{K}$ in the case of different support sizes a is non-singular. Thus, the solvability is not guaranteed for varying a.

In case of approximation, Eq. (11) can be extended to:

$$(\mathbf{K} + \lambda \mathbf{W}^{-1})\boldsymbol{\alpha} = \mathbf{q}_k \quad \text{with } \mathbf{W} = \text{diag}\{1/\sigma_1^2, ..., 1/\sigma_n^2\}, \tag{12}$$

where σ_i are the individual weights of the landmarks which represent landmark localization errors and λ is a general weighting parameter (see Section 2.1). Also in this case, the solvability of Eq. (12) is always guaranteed, since $\mathbf{W}$

is positive definite and a sum of two positive definite matrices also yields a positive definite matrix.

Efficiency. In comparison to the Gaussian or the inverse multiquadrics, neither exponential nor root functions have to be evaluated for the $\psi_{3,1}$-function, which is a polynomial. Also, depending on the size a of the support and the distribution of the landmarks $\mathbf{p}_i$ the matrix $\mathbf{K}$ is rather sparse (see also below). However, one has to note that the difference in efficiency between ψ and the Gaussian or the inverse multiquadrics depends on the number and the spatial distribution of landmarks.

Note, that landmarks with zero displacement, i.e. which is the case if the source landmark $\mathbf{p}_i$ and the target landmark $\mathbf{q}_i$ coincide, can be used to "fix" the transformation at these points. However, these "fixed" landmarks can be dropped when no other landmark with non-zero displacement is placed inside the radius of the compact support.

3.3. Comparison with the Gaussian

In Fig. 1, we compare the shape of the ψ-functions $\psi_{a,3,0}(r)$ and $\psi_{a,3,1}(r)$ with Gaussian. Like all positive definite functions, $\psi(r)$ has its maximum at $r = 0$.

For a given value of σ of the Gaussian, we computed a such that the integrals over both functions were equal. This yields:

$$a/3 = \sqrt{\pi/2}\sigma \Rightarrow a = \sqrt{\pi/2}\sigma.$$

The similarity of the graphs $\psi_{a,3,1}$ and the Gaussian is striking.

Having demonstrated the shape similarity between the ψ-functions and the Gaussian, we investigate the differences of the mathematical properties when used for registration. Suppose a registration task with 7 landmarks where 4 landmarks have been placed at the respective corners of the image which are fixed while 3 landmarks placed in the middle of the image have a non-zero displacement. The calculated matrices $\mathbf{K}$ in Eq. (11) are shown for $\psi_{a,3,1}$

with $a = 120$ in Eq. (13) and for the Gaussian with the corresponding $\sigma = 31.91$ in Eq. (14).

$$\mathbf{K}_{\psi_{3,1}} = \begin{pmatrix} 1 & 0 & 0 & 0 & 0 & 0 & 0 \\ 0 & 1 & 0 & 0 & 0 & 0 & 0 \\ 0 & 0 & 1 & 0 & 0 & 0.000825 & 0 \\ 0 & 0 & 0 & 1 & 0 & 0 & 0.0282 \\ 0 & 0 & 0 & 0 & 1 & 0 & 0 \\ 0 & 0 & 0.000825 & 0 & 0 & 1 & 0 \\ 0 & 0 & 0 & 0.0282 & 0 & 0 & 1 \end{pmatrix} \tag{13}$$

$$\mathbf{K}_{\mathrm{G}} = \begin{pmatrix} 1 & 2.85\times10^{-16} & 8.12\times10^{-32} & 2.85\times10^{-16} & 2.43\times10^{-06} & 6.07\times10^{-17} & 6.74\times10^{-11} \\ 2.85\times10^{-16} & 1 & 2.85\times10^{-16} & 8.12\times10^{-32} & 2.43\times10^{-06} & 4.92\times10^{-10} & 1.56\times10^{-19} \\ 8.12\times10^{-32} & 2.85\times10^{-16} & 1 & 2.85\times10^{-16} & 1.6\times10^{-11} & 0.00399 & 6.74\times10^{-11} \\ 2.85\times10^{-16} & 8.12\times10^{-32} & 2.85\times10^{-16} & 1 & 1.6\times10^{-11} & 4.92\times10^{-10} & 0.0292 \\ 2.43\times10^{-06} & 2.43\times10^{-06} & 1.6\times10^{-11} & 1.6\times10^{-11} & 1 & 0.000761 & 5.37\times10^{-05} \\ 6.07\times10^{-17} & 4.92\times10^{-10} & 0.00399 & 4.92\times10^{-10} & 0.000761 & 1 & 0.000116 \\ 6.74\times10^{-11} & 1.56\times10^{19} & 6.74\times10^{-11} & 0.0292 & 5.37\times10^{-05} & 0.000116 & 1 \end{pmatrix} \tag{14}$$

The matrix in Eq. (13) is sparse and can easily be separated into sub-matrices where only one entry per row and column appears, whereas matrix (14) is dense and cannot be separated. When instead using a truncated Gaussian (which is the case, when very small numbers are zero due to finite machine precision) the positive definiteness is no longer valid and thus, it is not guaranteed that the corresponding matrix is regular. Instead the matrix for $\psi_{3,1}$ in Eq. (13) is both sparse and regular and thus the linear system of equations is always solvable.

The reason why the matrix $\mathbf{K}$ corresponding to the truncated Gaussian is generally not positive definite can be explained as follows. A truncation of a function is obtained by multiplication with a box function. In the frequency domain this corresponds to a convolution with a sine-function. In the case of the Gaussian the Fourier transformation of the truncated function generally has negative values. From this directly follows that the truncated Gaussian cannot be positive definite (see Refs. [1,8]).

3.4. Preservation of topology

A major requirement for an elastic registration scheme is preservation of topology. Necessary conditions are that the function u is continuous and that the determinant of the Jacobian matrix must be positive at each point of the image ("locally 1-to-1" property) [3]:

$$\det(\nabla\mathbf{u}) > 0. \tag{15}$$

To prove the global univalence or "globally 1-to-1" property [3] of the transformation we use a theorem from Ref. [7]:

Theorem 1. *If $\mathbf{u} : \Omega \to \mathbb{R}^n$, where Ω is a closed rectangular region of $\mathbb{R}^n$, is differentiable mapping such that the Jacobian matrix $\nabla\mathbf{u}$ is a P-matrix for all x in Ω then $\mathbf{u}$ is univalent in Ω.*

Note that an $n \times n$ real matrix is said to be a P-matrix, if all its principal minors are positive.

We analyzed the Jacobian matrix for an isolated landmark $\mathbf{p}$ for our transformation function $\mathbf{u}$, which consists of an identity mapping plus the superposition of a local basis function. For an isolated landmark in the 2D case we have:

$$u_1(\mathbf{x}) = x + \Delta_1 \psi(\|\mathbf{x}-\mathbf{p}\|) \qquad u_2(\mathbf{x}) = y + \Delta_2 \psi(\|\mathbf{x}-\mathbf{p}\|), \tag{16}$$

where ψ is a local RBF, Δ_1 and Δ_2 are the displacement from the source landmark $\mathbf{p}$ to the target landmark $\mathbf{q}$ in x- and y-coordinate direction, respectively, and $\mathbf{p}$ is an arbitrary position of the landmark. Inserting Eq. (16) in Eq. (15), it follows:

$$\det(\nabla\mathbf{u}) = \frac{\partial u_1}{\partial x}\frac{\partial u_2}{\partial y} - \frac{\partial u_1}{\partial y}\frac{\partial u_2}{\partial x}$$

$$= \left(1 + \Delta_1\frac{\partial\psi}{\partial x}\right)\left(1 + \Delta_2\frac{\partial\psi}{\partial y}\right) - \Delta_1\Delta_2\frac{\partial\psi}{\partial y}\frac{\partial\psi}{\partial x} > 0$$

$$\Rightarrow \Delta_1\frac{\partial\psi}{\partial x} + \Delta_2\frac{\partial\psi}{\partial y} > -1$$

$$\Rightarrow \Delta_1\frac{\partial\psi}{\partial r}\frac{x - p_x}{\|\mathbf{x}-\mathbf{p}\|} + \Delta_2\frac{\partial\psi}{\partial r}\frac{y - p_y}{\|\mathbf{x}-\mathbf{p}\|} > -1$$

$$\Rightarrow \Delta_1\frac{\partial\psi}{\partial r}\cos\phi + \Delta_2\frac{\partial\psi}{\partial r}\sin\phi > -1,$$

where ψ stands for $\psi(\|\mathbf{x}-\mathbf{p}\|)$ and $r = \|\mathbf{x}-\mathbf{p}\|$. If we now set $\Delta = \max(\Delta_1, \Delta_2)$ we get for the worst case ($\phi = \pi/4$) in

Table 1
Minimum values of $(\partial\psi/\partial r)$

	$\psi_{a,3,1}$	$\psi_{a,3,2}$	Gaussian
$\left(\dfrac{\partial\psi}{\partial r}\right)_{min}$	$-\dfrac{135}{64}\dfrac{1}{a}$	$-2.50\dfrac{1}{a}$	$-\dfrac{1}{\sqrt{e}}\dfrac{1}{\sigma}$

2D:

$$\Delta\frac{\partial\psi}{\partial r} > -\frac{1}{\sqrt{2}}. \tag{17}$$

For the 3D case we obtain an analogous condition:

$$\det(\nabla\mathbf{u}) = 1 + \Delta_1\frac{\partial\psi}{\partial x} + \Delta_2\frac{\partial\psi}{\partial y} + \Delta_3\frac{\partial\psi}{\partial z} > 0.$$

If we again set $\Delta = \max(\Delta_1, \Delta_2, \Delta_3)$ we obtain for the worst case in 3D:

$$\Delta\frac{\partial\psi}{\partial r} > -\frac{1}{\sqrt{3}}. \tag{18}$$

With the conditions (17) and (18) it can be shown that all principal minors of the Jacobian are positive for the 2D and 3D case, respectively. It follows that the transformations (defined for 2D in Eq. (16)) preserve the topology if Eqs. (17) and (18) hold. The minimum of $(\partial\psi/\partial r)$ depends on the locality parameter either a or σ. Table 1 summarizes $(\partial\psi/\partial r)$ for different local basis functions. With the help of Table 1 and Eqs. (17) and (18), the conditions for the locality parameter a and σ can be derived. They are listed in Table 2.

These conditions are valid only for isolated landmarks for which no other landmark is placed within the radius a of the support. For landmarks with intersecting support regions the minimal value of a depends also on the positions of the landmarks $\mathbf{p}_i$ which leads to a much more complicated calculation. Nevertheless, Table 2 is a good reference and gives a clue for choosing a value for the locality parameter a.

As our experiments (see below) revealed, the setting of the locality parameter is related to the spatial distribution of landmarks. Further investigations are necessary to clarify this relationship. As one conclusion from our experiments, one can say that the closer the landmarks are placed the smaller the locality parameter can be chosen. In our experiments, we kept the parameter a as small as possible such as to maximize the locality of the transformation.

Table 2
Minimum a and σ for given displacement Δ

Dimension	$\psi_{a,3,1}$	$\psi_{a,3,2}$	Gaussian
$d = 2$	$a > 2.98\Delta$	$a > 3.54\Delta$	$\sigma > 0.86\Delta$
$d = 3$	$a > 3.66\Delta$	$a > 4.33\Delta$	$\sigma > 1.06\Delta$

4. Experimental results

We now present registration results for synthetic and tomographic images using the elastic registration approach based on RBFs with compact support introduced in Section 3. Here, we confine ourselves to the interpolation case. We first demonstrate the applicability of this approach for simple objects, which shift or scale in elastic material. Second, we show experimental results for registering a pre-operative image with the corresponding post-operative image after tumor resection. Since with our approach only local misregistrations can be handled, prior global registration is necessary, e.g. by applying a rigid or affine transformation.

In Fig. 2, we demonstrate the registration of objects embedded in elastic material that change their position or form. Landmarks are placed at the outlines. These experiments simulate typical medical cases, where image parts shift and either shrink or grow as it happens in cases of, e.g. tumor growth or tumor resection. The grids in Fig. 2 represent 301×301 pixels and they are transformed using 24 landmarks as indicated in Fig. 2(a) and (d). Landmarks of the source and the target image are marked by a box ($\square$) and a circle ($\bigcirc$), respectively. The distance between two adjacent gridlines is 15 pixels. Parts of the grids which represent the areas to be registered are colored gray. Source and target landmarks are both shown in the left images. In Fig. 2(a), the landmarks were shifted 20 pixels on both the x- and y-axes to the bottom right. Fig. 2(b) shows the registration result using $\psi_{3,1}$ with a support of $a = 90$ which we found experimentally to be visually the best. We started with the value from Table 2 $a = 60$ and proceeded to $a = 120$ in steps of 10. With growing distance outside the square the influences of the landmarks decrease monotonically. The margin where the transformation function reduces to the identity is marked as gray curve. In Fig. 2(d) we demonstrate a scaling example. Fig. 2(e) shows the registration result for $a = 50$ which we found to be the smallest value with good results while testing values from a range of 30–120 (Table 2 gives a clue of 45). The registration result is mainly limited to the square.

For comparison, we registered both images using also the thin-plate spline approach, see Fig. 2(c) and (f). To prevent an overall shift, we have added 4 landmarks in the corners of the images which all have a zero displacement. It can be seen that the registration is global and affects the whole image. Over the whole image the deformation is smooth. Using the ψ-functions, there is a tradeoff between the smoothness and the locality of the registration: the larger the area of influence the smoother is the registration and vice versa. Actually, using ψ-functions with a very large support ($a > \approx 1000$) for registration, the results resemble very much those registered with the TPS approach as shown in Fig. 3.

Fig. 4 shows an experiment with tomographic images where a tumor in a pre-operative image has to be registered

(a) Shift of a square   (b) Result using $\psi_{90,3,1}$ (c) Result using TPS

(d) Scaling of a square   (e) Result using $\psi_{50,3,1}$ (f) Result using TPS
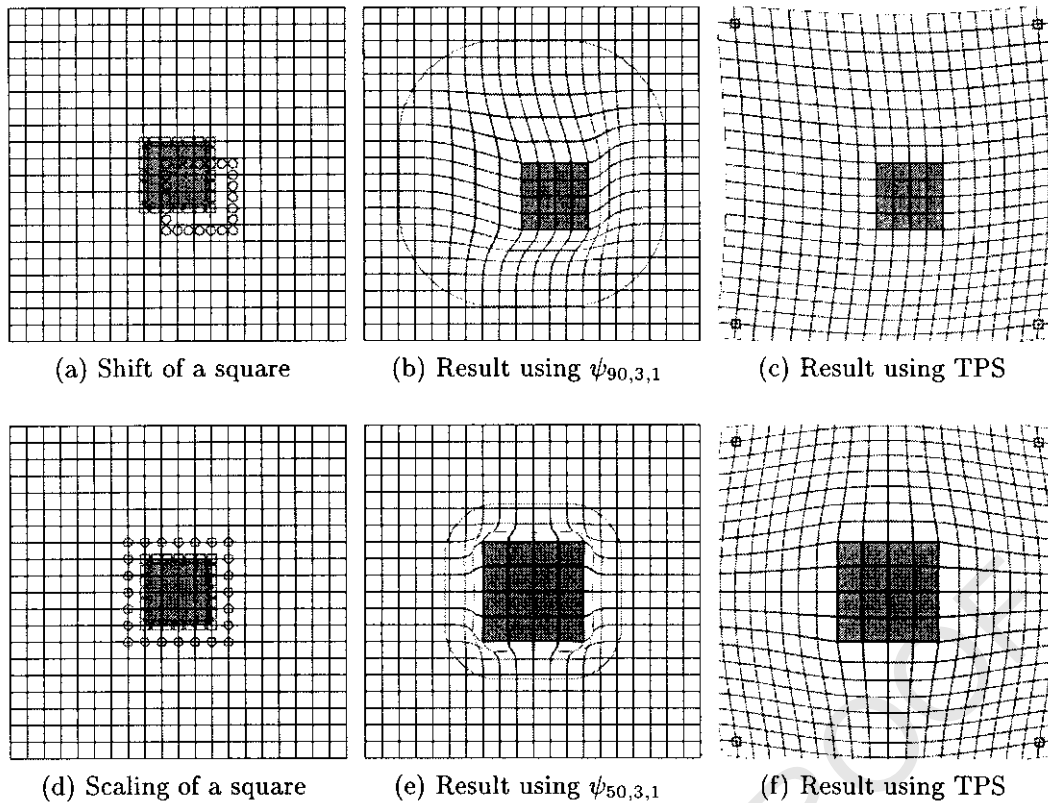
Fig. 2. Local elastic registration using $\psi_{3,1}$ as RBF: (a) shift and (d) isotropic scaling of a square; (b) and (e) show registration results together with the influence area where elastic deformations occur; (c) and (f) show registration results with thin-plate splines for comparison.

with the corresponding resection area in the post-operative image. An application scenario is the registration of pre-operative tomographic images of high resolution (e.g. MR) with intra-operative images of worse quality (e.g. CT or MR). The aim is to correct the pre-operatively acquired image such that it agrees with the current anatomical situation. For demonstration purposes, in our case, we use a post-operative image instead of an intra-operative image. The source image 4(a) and the target image 4(b) are corresponding slices of rigidly transformed 3D MR datasets. In Fig. 4(a), landmarks are placed at the margin of the brain tumor as well as at the outer and inner part of the skin in the vicinity of the tumor. Corresponding target landmarks are shown in Fig. 4(b). The tumor itself corresponds to the resection area. The correspondences between the contours of the skin, the brain, and the tumor have been determined

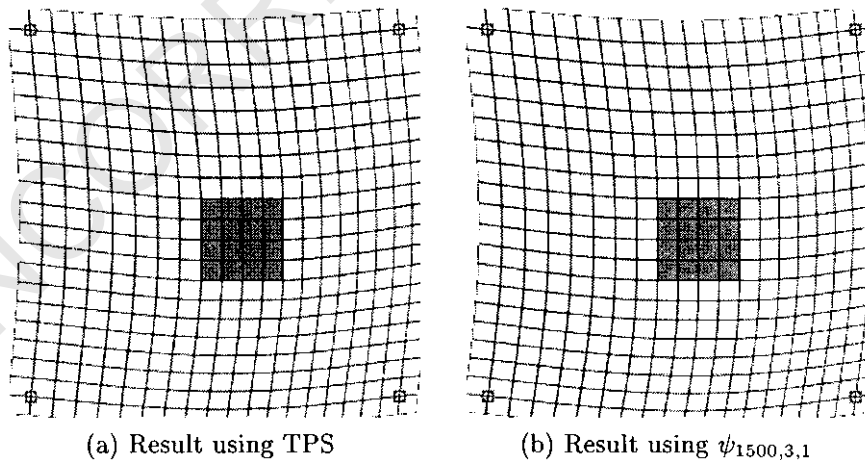(a) Result using TPS   (b) Result using $\psi_{1500,3,1}$

Fig. 3. Comparison of $\psi_{3,1}$ with large support and TPS: (a) registration result using TPS (same as Fig. 2(c)) and (b) registration result using $\psi_{3,1}$ with $a = 1500$.

(a) Source

(b) Target

(c) Result using $\psi_{60,3,1}$
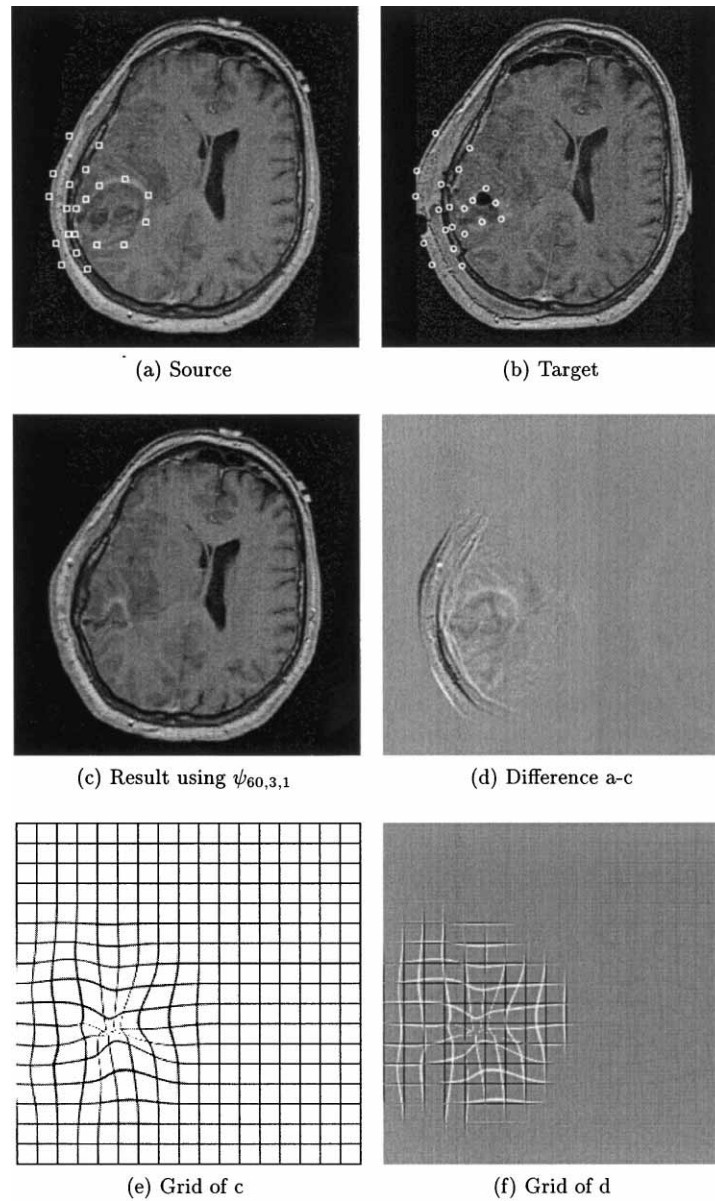
(d) Difference a-c

(e) Grid of c

(f) Grid of d

Fig. 4. Registration of a tumor with its resection area: (a) pre-operative image; (b) post-operative image; (c) registration result; (d) difference between (a) and (c); (e) and (f) same as (c) and (d) for an underlying grid.
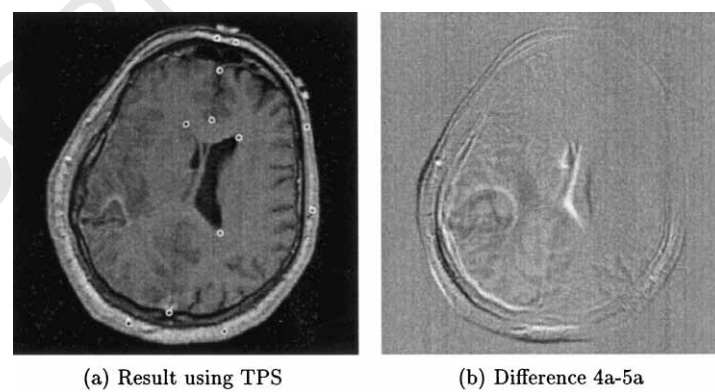

(a) Result using TPS

(b) Difference 4a-5a

Fig. 5. Registration of a tumor with its resection area. Comparison with TPS: (a) registration result using thin-plate splines with additional landmarks and (b) difference between Figs. 4(a) and 5(a).

(a) Source image   (b) Target image   (c) Result using $\psi_{60,3,1}$

(d) Slice 32 of source image   (e) Slice 32 of registration result

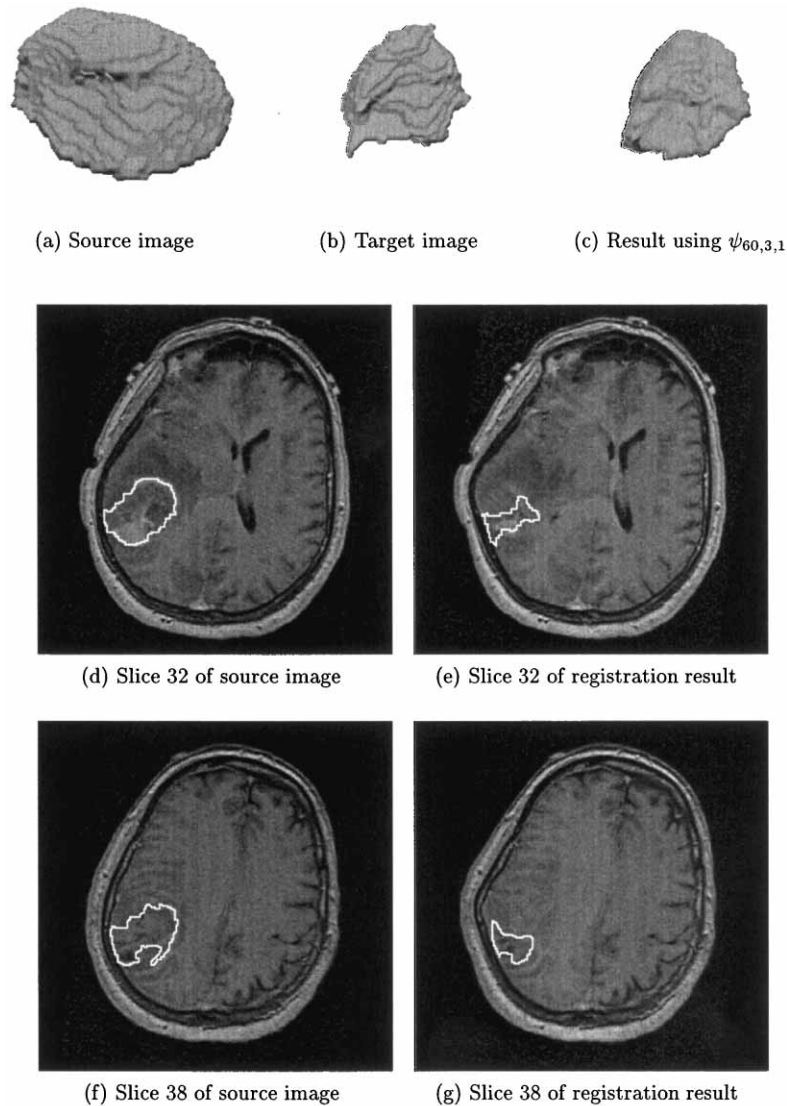(f) Slice 38 of source image   (g) Slice 38 of registration result

Fig. 6. 3D Registration of a tumor with its resection area. (a) and (b) 3D segmentation of the tumor and the resection area as well as (c) 3D registration result showing the transformed tumor only. (d) and (f) show different slices of the 3D source image, (e) and (g) the corresponding slices of the 3D registration result.

through the use of a snake algorithm [10] (see also Ref. [12]). Out of these correspondences we have interactively selected 21 pairs of landmarks shown in Fig. 4(a) and (b). Note, that there is also a significant brain shift at the top of Fig. 4(b), which will not be considered here. For this registration problem, a reduction of the influence of the registration scheme far off the area of interest is necessary and thus the locality of the registration w.r.t. tumor is desired.

In Fig. 4(c), the transformation result is shown using $\psi_{3,1}$ with $a = 60$ as RBF. Since the maximum displacement in one coordinate direction of the landmark set is 17, the reference value is $a \approx 50$ (Table 2). Our experiments revealed that a value of $a = 60$ yielded quite good results, while being close to the reference value and thus ensuring a rather local registration result. To assess the form of the transformation, we have applied it to a regular grid which we show in Fig. 4(e). It can be seen that the tumor is registered to the

resection area while the region around the tumor is shifted towards the resection area. The reduced influence of the transformation is demonstrated in Fig. 4(d) and (f) where the source image was subtracted from the registration result. To demonstrate the differences to RBFs without compact support, we applied the thin-plate spline approach to the same problem as shown in Fig. 5(a). Note, that additional landmarks in other parts of the image are necessary to prevent deformations there. Although we have added 11 of these additional landmarks, thin-plate spline transformations are rather global as it is best seen in the difference image in Fig. 5(b). Here, the deformations are not limited on the tumor area.

In Fig. 6, we demonstrate the applicability of our approach for the case of a 3D registration problem. The outlines of the tumor as well as of the resection area have been determined manually. 40 landmarks have been used

and the correspondences have been determined by simply intersecting rays going through the common geometric center point with the corresponding surfaces. First, we segmented the tumor and the resection area as shown in Fig. 6(a) and (b). The registration result is shown in Fig. 6(c), which is quite similar to the target image. Fig. 6(d) and (f) shows exemplarily two slices of the 3D dataset together with the outlines of the tumor. The registration result for the same slices is shown in Fig. 6(e) and (g), respectively. Also here, the deformation is limited to an area around the tumor.

5. Conclusion

We have proposed an approach to elastic registration which utilizes positive definite functions of compact support as RBFs. In comparison to the truncated Gaussian, they have the advantage that the corresponding matrix for solving the system of equations is always regular, thus the system of equations is always solvable. In comparison to thin-plate spline based elastic registration [2,14] with our approach, we have a significant reduction of the global influence, i.e. the influence of a landmark on the registration result is limited to a circle in 2D or, respectively, to a sphere in 3D. Therefore, the registration is locally constrained which especially allows us to deal with local changes in medical images. The synthetic experiments have shown that object deformations can well be locally registered using landmarks placed at the outlines of the objects. Experiments with 2D and 3D tomographic images have demonstrated the applicability of our approach to registering pre-operative images with post-operative images in the case of tumor resection. Further investigations are necessary to determine appropriate landmark distributions and correspondences as well as support sizes of the RBFs for registration problems at hand.

5. Uncited References

[18].

References

[1] N. Arad, D. Reisfeld, Image warping using few anchor points and radial functions, Computer Graphics Forum 14 (1) (1995) 35–46.

[2] F.L. Bookstein, Principal warps: thin-plate splines and the decomposition of deformations, IEEE Transactions on Pattern Analysis and Machine Intelligence 11 (6) (1989) 567–585.

[3] G.E. Christensen, R.D. Rabbitt, M.I. Miller, S.C. Joshi, U. Grenander, T.A. Coogan, D.C. van Essen, Topological Properties of Smooth Anatomic Maps, in: Y. Bizais, C. Barillot, R.D. Paola (Eds.), Information Processing in Medical Imaging, 14th International Conference, Ile de Berder, France, June, vol. 3, Kluwer, Dordrecht, 1995, pp. 101–112.

[4] A.C. Evans, W. Dai, L. Collins, P. Neelin, S. Marrett, Warping of a computerized 3-D atlas to match brain image volumes for quantitative neuroanatomical and functional analysis, in: M.H. Loew (Ed.), Proc. SPIE 1445, Medical Imaging V: Image Processing, pp. 236–246, San Jose, CA, 1991.

[5] M. Fornefett, K. Rohr, H.S. Stiehl, Elastic Registration of Medical Images Using Radial Basis Functions with Compact Support, Proc. IEEE Int. Conf. on Computer Vision and Pattern Recognition (CVPR'99), Fort Collins, CO, June 23–25, IEEE Computer Society, 1999 (pp. 402–407).

[6] M. Fornefett, K. Rohr, H.S. Stiehl, Radial Basis Functions with Compact Support for Elastic Registration of Medical Images, in: F. Pernuš, S. Kovacic, H.S. Stiehl, A. Viergever (Eds.), Proc. Int. Workshop on Biomedical Image Registration (WBIR'99), Bled, Slovenia, 30–31 August, Slovenian Pattern Recognition Society, Slovenia, 1999, pp. 173–185.

[7] D. Gale, H. Nikaido, The Jacobian matrix and global univalence of mappings, Mathematische Annalen 159 (1965) 81–93.

[8] A. Goshtasby, Image registration by local approximation methods, Image and Vision Computing 6 (1988) 255–261.

[9] R.L. Hardy, Multiquadric equations of topography and other irregular surfaces, Journal of Geophysical Research 76 (8) (1971) 1905–1915.

[10] M. Kass, A. Witkin, D. Terzopoulos, Snakes: active contour models, International Journal of Computer Vision 1 (4) (1988) 321–331.

[11] J.A. Little, D.L.G. Hill, D.J. Hawkes, Deformations incorporating rigid structures, Computer Vision and Image Understanding 66 (2) (1997) 223–232.

[12] W. Peckar, C. Schnörr, K. Rohr, H.S. Stiehl, Parameter-free elastic deformation approach for 2-D and 3-D registration using prescribed displacements, Journal of Mathematical Imaging and Vision 10 (1999) 143–162.

[13] K. Rohr, M. Fornefett, H.S. Stiehl, Approximating thin-plate splines for elastic registration: integration of landmark errors and orientation attributes, in: A. Kuba, M. Šámal, A. Todd-Pokropek (Eds.), Proc. 16th Int. Conf. on Information Processing in Medical Imaging (IPMI'99), Visegrád, Hungary, June 28–July 2, Lecture Notes in Computer Science, vol. 1613, Springer, Berlin, 1999, pp. 252–265.

[14] Rohr, H.S. Stiehl, R. Sprengel, W. Beil, T.M. Buzug, J. Weese, M.H. Kuhn, Point-based elastic registration of medical image data using approximating thin-plate splines, in: K.H. Höhne, R. Kikinis (Eds.), Proc. Fourth Int. Conf. on Visualization in Biomedical Computing (VBC'96), Hamburg, Germany, 22–25 September, Lecture Notes in Computer Science, vol. 1131, Springer, Berlin, 1996, pp. 297–306.

[15] D. Ruprecht, H. Müller, Free form deformation with scattered data interpolation methods, Computing Supplementum 8 (1993) 267–281.

[16] O. Soligon, A. Le Mehaute, C. Roux, Facial expressions simulation with Radial Basis Functions, in: International Workshop on Synthetic–Natural Hybrid Coding and Three Dimensional Imaging (IWSNHC3DI'97), Rhodes, Greece, pp. 233–236, 5–9 September 1997.

[17] H. Wendland, Piecewise polynomial, positive definite and compactly supported radial functions of minimal degree, Advances in Computational Mathematics 4 (1995) 389–396.

[18] H. Wendland, Konstruktion und Untersuchung radialer Basisfunktionen mit kompaktem Träger. PhD thesis, Universität Göttingen, Juni 1996.